

CHAPTER 1

PHOTOVOLTAIC CELLS AND PHENOMENA

1.1. Overview

A material (or device) is said to be “photovoltaic” when exposure of the material to light that can be absorbed by the material is able to transform the energy of the light photons into electrical energy in the form of a current and voltage. The concept is simple and the number of materials that are able to exhibit photovoltaic characteristics is large. What is not large, however, is the number of such materials or devices that are able to make the transformation of solar radiation to electrical energy with high efficiency, of the order of 20%, at low cost, and with high stability under operation.

The development of photovoltaic cells can be dated originally to Becquerel’s discovery in 1839 of a photovoltage produced by the action of light on an electrode in an electrolyte solution (Becquerel, 1839). About 40 years later, Adams and Day observed the photovoltaic effect in selenium (Adams and Day, 1877). Solar efficiencies of about 1% characterized selenium and copper oxide cells by about 1914. The modern era of semiconductor photovoltaics started in 1954 when Chapin, Fuller and Pearson obtained a solar efficiency of 6% for a silicon junction cell (Chapin *et al.*, 1954), a value that was increased to 14% by 1958, and to 28% by 1988 (Verlinden *et al.*, 1988). The year 1954 also dates the announcement of the first all-thin-film cell composed of a $\text{Cu}_x\text{S}/\text{CdS}$ junction (Reynolds *et al.*, 1954) with an efficiency of 6%, later increased to over 9% (Bragagnolo *et al.*, 1980), which unfortunately had the stability problems described below. The first mention of a cell based on GaAs was for a 4% p - n homojunction in 1956 (Jenny *et al.*, 1956); later developments were to produce cells with efficiencies greater than 30%, as discussed in Chapter 4. Concern about energy resources motivated a strong surge of interest in solar cells for terrestrial applications in the early 1970’s. In spite of the fact that the 1980’s and ’90s have been a period in which public and government support for photovoltaics have been underemphasized, considerable activity and progress in research and development of solar cells has continued.

The Photovoltaic Process

The basic concept of the photovoltaic process is also simple. When light with photon energy greater than the band gap is absorbed by a semiconductor material, free electrons and free holes are formed by optical excitation in the semiconductor. The crucial characteristic needed for the photovoltaic effect is the presence of some kind of internal electric field (from any of a variety of causes: e.g. different doping in different regions, contacts, surfaces, etc.) that is able to separate the freed electrons and holes so that they can pass out of the material into the external circuit before they recombine with one another. The flow of carriers into the external circuit constitutes a reverse electrical current density, J amp cm^{-2} , which, under short-circuit conditions, is known as the short-circuit current density, J_{sc} . (For consistency, in this book the term current will always mean current density J unless specifically stated otherwise. The total current $I = JA$, where A is the area through which the current flows.) At the same time, the separation of the charges sets up a forward

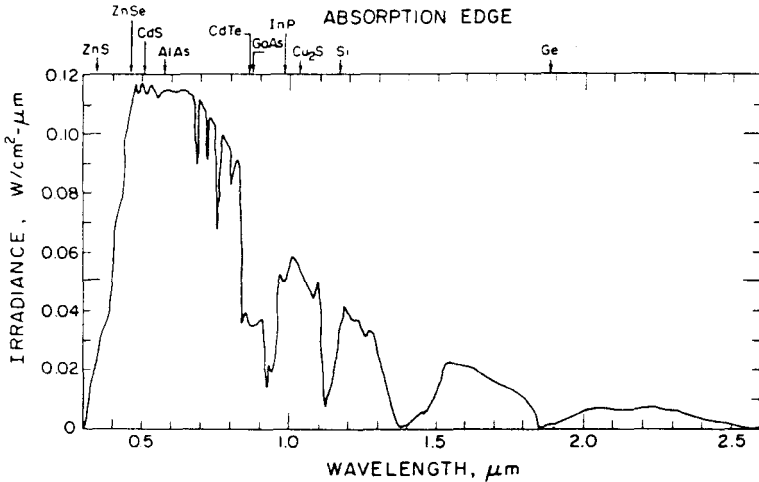


Fig. 1.1. Average solar spectrum at the surface of the earth, with the band gaps of various semiconductors indicated. As discussed in this chapter, a homojunction or a front-wall heterojunction will absorb all the solar spectrum to the left of the indicated absorption edge for a particular material. A back-wall heterojunction will absorb the solar spectrum between the two band gaps of the materials making up the heterojunction. (Reprinted from R. H. Bube, "Solar Cells" in *Handbook on Semiconductors. Device Physics*. Vol. 4C. C. Hilsum, ed., 1993, p. 797, with kind permission from Elsevier Science — NL, Sara Burgerhartstraat 25, 1055 KV Amsterdam, The Netherlands.)

potential difference between the two ends of the material, ϕ , which under open-circuit conditions is known as the open-circuit voltage, ϕ_{oc} . The polarity of the open-circuit voltage, therefore, is such as to drive electrons (holes) in the opposite direction (the forward-bias direction) to that of the electron (hole) motion in the short-circuit current. Specific examples of photovoltaic systems are described in more detail in following sections of this chapter.

Maximizing Photovoltaic Performance

It is desirable to maximize both J_{sc} and ϕ_{oc} . In order to maximize J_{sc} , it is desirable (1) to absorb as much of the incident light as possible, i.e. to have a small band gap with high absorption over a wide energy range, and (2) to

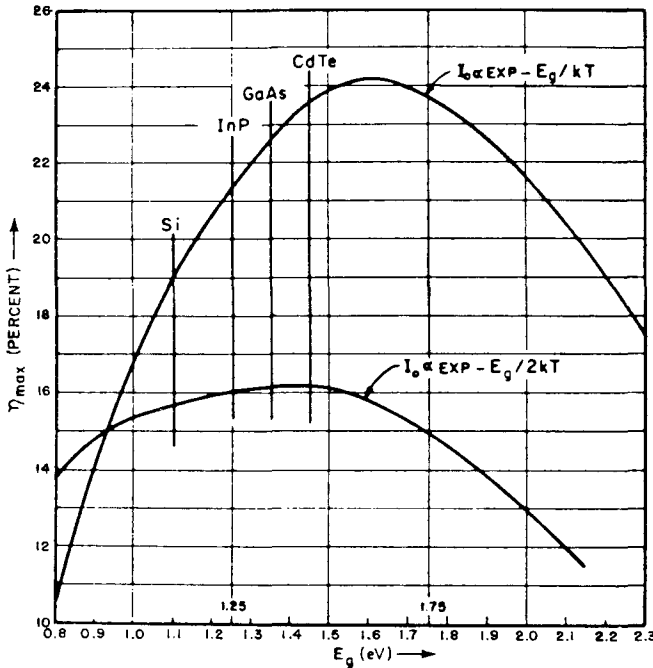


Fig. 1.2. An early calculation of the theoretical solar efficiency versus semiconductor band gap for ideal $p-n$ homojunction cells with no surface recombination loss. Curves are shown for two different junction transport mechanisms: (top) $A = 1$ for injection dominated current and (bottom) $A = 2$ for recombination in the depletion layer. (Reprinted with permission from J. J. Loferski, *J. Appl. Phys.* **27**, 777 (1956). Copyright 1956, American Institute of Physics.)

4 Photovoltaic Materials

have material properties such that the photoexcited electrons and holes are able to be collected by the internal electric field and pass into the external circuit before they recombine, i.e. a material with a high minority carrier lifetime and mobility. In order to maximize ϕ_{oc} , it is also preferred to have the forward current driven by the photo-induced potential difference be as small as possible since this current will reduce the potential difference set up by light. The details of this forward current depend critically on the actual mechanisms of transport involved, but in general the forward current varies inversely as the band gap of the material.

From these two purely qualitative considerations, therefore, it may be concluded that there will be an optimum band gap or band gap range for

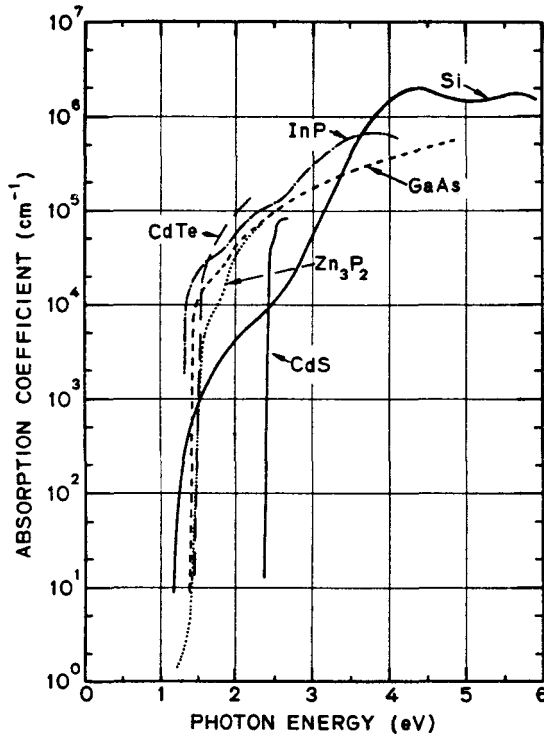


Fig. 1.3. Optical absorption coefficients of various single-crystal semiconductors commonly used in photovoltaic devices. (Reprinted with permission from A. L. Fahrenbruch and R. H. Bube, *Fundamentals of Solar Cells: Photovoltaic Solar Energy Conversion*, Copyright 1983, Academic Press, Orlando, FL.)

maximizing both J_{sc} and ϕ_{oc} , and hence the efficiency of the photovoltaic device itself. For interaction with the solar spectrum (see Fig. 1.1), this optimum band gap range lies approximately between 1.2 and 1.8 eV. The results of one of the first calculations of the dependence of efficiency on band gap for two different types of junction current are pictured in Fig. 1.2 (Loferski, 1956). Details of the concepts described in the figure caption are discussed later in this chapter. For comparison, Fig. 1.3 shows the dependence of optical absorption coefficients on photon energy for various single-crystal semiconductors used in photovoltaic devices (Fahrenbruch and Bube, 1983).

Description of Solar Spectrum

As shown in Fig. 1.1, the sun is a complex radiator with a spectrum that can be approximated by the spectrum of a 6050 K black body. This spectrum is then modified by temperature variations across the sun's disk, the effects of the solar atmosphere, Fraunhofer absorption lines, and the path length of the radiation through the earth's atmosphere, where the primary effects are due to water content, turbidity, ozone, cloudiness, and ground reflection.

For terrestrial applications, the path length through the atmosphere is of fundamental importance. This path length can be conveniently described in terms of an equivalent "air mass", m_r . If a zenith angle z is defined as the angle from the normal to the plane containing the horizon circle, which describes the declination of the sun, the path length for a zenith angle z is just $\sec z$ times the path length for $z = 0$, and the air mass m_r , is defined as $m_r = \sec z$. Specific solar spectra are labeled AMm_r (read: air mass m_r). $AM0$ corresponds to the solar spectrum in outer space; $AM1$ to the solar spectrum at the earth's surface for the sun overhead. $AM2$ corresponds to an approximately average solar spectrum at the earth's surface.

Simplest Photovoltaic Device

In order to make these introductory concepts more specific, let us consider the simplest photovoltaic device and the mathematical description of the electrical properties of such a device. In subsequent sections of this chapter, we summarize some of the possible variations and complications in more detail. Here we use the simple equivalent circuit for a photovoltaic cell as shown in Fig. 1.4, including a current generator corresponding to photoexcitation, a diode containing the internal electric field necessary for driving photoexcited carriers to the external circuit, a series resistance, R_s , and a parallel resistance, R_p . We

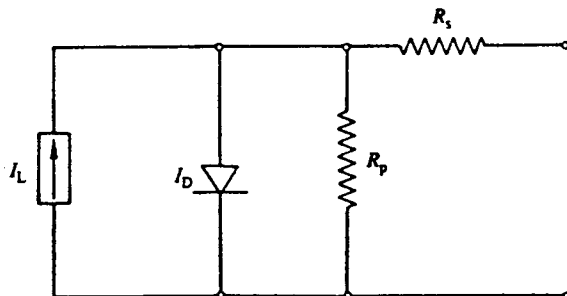


Fig. 1.4. Simple equivalent circuit for a photovoltaic cell, including a current generator with total light current I_L , a diode with total dark current I_D , a series resistance R_s , and a parallel resistance R_p . (Reprinted with permission from R. H. Bube, *Photoelectronic Properties of Semiconductors*, Copyright 1992, Cambridge University Press.)

make the model even simpler by considering at this point an “ideal device” with $R_s = 0$ and $R_p = \infty$. If we make the simple assumption that the current generated by light can simply be added to the current flowing in the dark (“superposition”), then the current density J flowing in the device in the presence of photoexcitation can be expressed as

$$J = J_o[\exp(q\phi/AkT) - 1] - J_L \quad (1.1)$$

Here the first term on the right of Eq. (1.1) is the forward current driven by the voltage ϕ , and the second term is the reverse current associated with photoexcitation. J_o is often called the “reverse saturation current” of the diode, the value of J in the dark for large negative values of ϕ in ideal junctions, which depends on the actual transport mechanism for the diode current (J_o is often called simply the “pre-exponential coefficient” in practical devices for which reverse saturation may not occur), and A is the so-called “ideality factor” that has a value depending on the mechanism of the junction transport (e.g., $A = 1$ if the transport process is diffusion, $A \approx 2$ if the transport process is recombination in the depletion region). Typical variations of total current I in both the dark and the light as a function of ϕ are given in Fig. 1.5. If the voltage is zero (short-circuit condition), then of course there is zero current in the dark, but in the light we have

$$J_{sc} = -J_L \quad (1.2)$$

and the short-circuit current is controlled only by the photoinduced current generation and the recombination processes. If the total current under

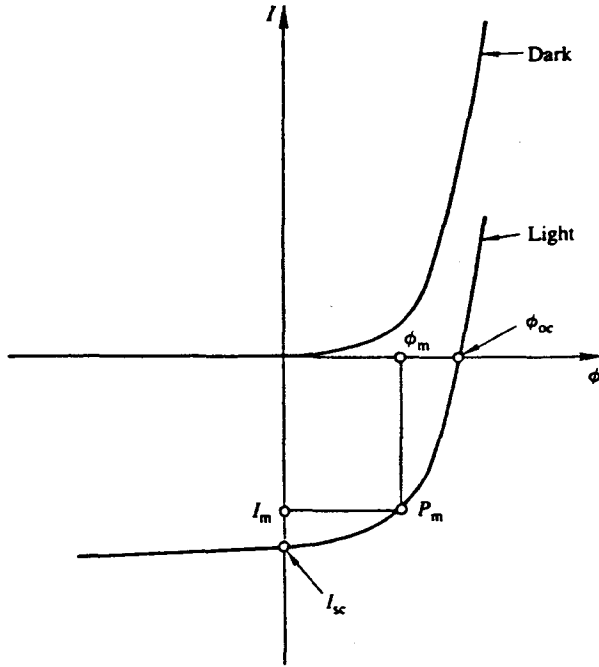


Fig. 1.5. Typical idealized total light and dark current versus voltage curves for a photovoltaic cell in which the principal cell parameters do not depend on photoexcitation, showing the open-circuit voltage ϕ_{oc} , the short-circuit current I_{sc} , and the maximum power point P_m . (Reprinted with permission from A. L. Fahrenbruch and R. H. Bube, *Fundamentals of Solar Cells: Photovoltaic Solar Energy Conversion*, Copyright 1983, Academic Press, Orlando, FL.)

illumination is zero (open-circuit condition), then solution of Eq. (1.1) for $J = 0$ gives

$$\phi_{oc} = (AkT/q) \ln[(J_L/J_o) + 1] \quad (1.3)$$

Thus the open-circuit voltage is controlled by the current generation and recombination processes, but also by the nature of the junction transport currents depending on A and J_o . Combination of Eqs. (1.2) and (1.3) shows that the relation between J_{sc} and ϕ_{oc} is given by

$$J_{sc} = J_o[\exp(q\phi_{oc}/AkT) - 1] \quad (1.4)$$

which is exactly similar to Eq. (1.1) for J versus ϕ in the dark for this ideal junction device. The equivalence of these two dependences is a basic test for the absence of any light-related changes in the parameters entering the equations.

Photovoltaic Efficiency

Since photovoltaic efficiency is of central importance, we see next how this efficiency is expressed in terms of this simple model. The efficiency of a photovoltaic solar cell is a maximum when the product of the current density J and the voltage ϕ is a maximum. The efficiency η itself can be expressed as

$$\eta = P_m/P_{\text{rad}} = J_m\phi_m/P_{\text{rad}} = J_{sc}\phi_{oc}ff/P_{\text{rad}} \quad (1.5)$$

where P_{rad} is the total radiation power incident on the cell, and ff is called the fill factor; ff is a measure of the “squareness” of the light J - ϕ curve, as shown in Fig. 1.5. J_m and ϕ_m are respectively the values of current density and voltage at the condition corresponding to maximum power. The definition of the fill factor ff can be obtained from Eq. (1.5),

$$ff = J_m\phi_m/J_{sc}\phi_{oc} \quad (1.6)$$

The value of ϕ_m can be obtained by multiplying Eq. (1.1) by ϕ and maximizing the power with respect to ϕ .

$$\phi_m = \phi_{oc} - (AkT/q) \ln[(q\phi_m/AkT) + 1] \quad (1.7)$$

which can be solved iteratively for ϕ_m . Once a value for ϕ_m has been obtained, the value of J_m , and hence the maximum power $P_m = J_m\phi_m$, can be obtained from Eq. (1.1) by substituting $\phi = \phi_m$. The fill factor for a junction describable by Eq. (1.4) is a function of A and ϕ_{oc} , increasing with decreasing A and increasing ϕ_{oc} (Lindmayer, 1972).

Figure 1.6 gives general insights into the factors that determine the efficiency in an actual photovoltaic solar cell. The figure shows the various components to the loss of efficiency in a standard single-crystal silicon cell for irradiation by sunlight. Specific numbers depend, of course, on the details of the material and the solar cell, and those given here are intended to be primarily illustrative. The analysis is similar to that carried out by Wolf (1971). Starting from the top of the diagram down:

- (1) Some of the cell area is obscured by the current-collecting grid, thus reducing the effective cell area: 4% loss;
- (2) some of the incident photons are reflected and not absorbed: 2% loss;
- (3) some of the photons are absorbed in spurious absorption processes such as at antireflection coatings, at defects, etc., which do not lead to free carriers: 1% loss;

REFLECTION LOSS	2.0%
SPURIOUS ABSORPTION	1.0%
GRID COVERAGE	4.0%
$h\nu < E_g$	18.8%
$h\nu > E_g$	29.2%
$\eta_Q = 0.90$	4.5%
$E_g > qV_{oc}$	19.2%
$ff = 0.78$	4.7%
$n_s = 16.6\%$	

Fig. 1.6. Power loss chart for a silicon cell showing the percentage of total input power P_{rad} lost to each of the loss mechanisms. Values of $J_o = 5 \times 10^{-12}$ A cm $^{-2}$ and $A = 1$ are assumed. (Reprinted with permission from A. L. Fahrenbruch and R. H. Bube, *Fundamentals of Solar Cells: Photovoltaic Solar Energy Conversion*, Copyright 1983, Academic Press, Orlando, FL.)

- (4) some of the incident photons have an energy less than the band gap of the semiconductor ($h\nu < E_g$), and hence have insufficient energy to produce free carriers in the absorbing material: 18.8% loss;
- (5) some of the absorbed photons have an energy larger than the band gap E_g of the absorbing material; the excess energy ($h\nu - E_g$) is non-usefully dissipated in producing hot carriers which transform the light energy to heat as the carriers thermalize to near the band edge: 29.2% loss;
- (6) not every photoexcited free carrier is collected by the internal electric field; this is expressed by the quantum efficiency $\eta_Q < 1$: if $\eta_Q = 0.90$, this amounts to a 4.5% loss;
- (7) in general the band gap $E_g > q\phi_{oc}$, i.e., the energy used to create the free carriers ($h\nu \geq E_g$) is greater than the energy associated with the open-circuit voltage, and there is therefore an energy loss of 19.2%;
- (8) finally in a real solar cell forward-biased to ϕ_m , with finite R_s and R_p , the fill factor $ff < 1$: if $ff = 0.78$, this amounts to a 4.7% loss.

Given the various estimates listed here, the cell efficiency is finally 16.6%. Losses (1) to (3), and (6) to (8), can be reduced by careful material control and cell design. Losses (4) and (5) are difficult to avoid with simple solar cells, but more complicated structures (graded gap or multijunction structures) can be designed to help here as well. Photovoltaic cells with efficiency over 30% have been designed and produced.

Summary of Important Materials Properties

We now summarize the most significant materials properties that are important for the preparation of high efficiency photovoltaic solar cells. Rothwarf (1987) has listed some twenty to thirty materials and processing related parameters that must be controlled and optimized for maximizing solar-cell performance.

- (1) Band gap of the absorbing material. The band gap of the absorbing material must be small enough to allow absorption of an appreciable portion of the solar spectrum, and at the same time large enough to minimize the reverse saturation junction current density J_o .
- (2) Diffusion length of minority carriers. The diffusion length of minority carriers must be as large as possible so that carriers excited by light some distance from the actual semiconductor junction will be able to diffuse to the junction and be collected before they recombine with carriers of the opposite sign. The diffusion length of minority carriers L_{\min} is given by $L_{\min} = (D_{\min}\tau_{\min})^{1/2} = [(kT/q)(\mu\tau)_{\min}]^{1/2}$, where D_{\min} is the diffusion constant, τ_{\min} is the lifetime, and μ_{\min} is the mobility, for minority carriers. It is desired, therefore, to have a material in which the minority carriers have as large a mobility and lifetime as can be obtained. The value of the mobility is more or less determined by the choice of material and does not vary over a wide range. The value of the lifetime, however, is very sensitive to a variety of phenomena in the bulk and at the surface that contribute to recombination of photoexcited carriers. Optimization of efficiency must include solar cell growth and deposition conditions that maximize the minority carrier lifetime. Cell design must include photoexcitation of minority carriers within a diffusion length of the collecting junction.
- (3) Desirable junction properties. The actual junction structure and composition determines the magnitude of the junction transport current density J_o and of the ideality factor A . Formation of the semiconductor junction must be carefully controlled, therefore, to produce junctions with as low a junction current as possible. Various typical mechanisms for the junction current are summarized in Sec. 1.4.

- (4) In the simple analysis of this section, we have assumed that $R_s = 0$ and $R_p = \infty$ in Fig. 1.4. In real solar cells, however, finite values of these two resistances will be present and can be a major factor, particularly in determining the effective value of the fill factor ff . Contributions to the series resistance R_s can arise both from the resistance of the semiconductor bulk and from the contact resistance to the semiconductor to complete the circuit. Problems involving semiconductor doping and control of contact resistance can play a significant role in some cases. The parallel resistance R_p can be reduced by grain boundaries or other defects that enhance forward junction current and contribute to an increase in J_o and a decrease in ϕ_{oc} . In polycrystalline thin film solar cells, grain boundaries at the junction interface can critically affect junction transport properties.
- (5) Solar cells are intended for use in exposed areas for long periods of time without failure. This means that a variety of phenomena that might lead to a decrease in cell efficiency with time of exposure must be carefully considered. In some cases, as we shall see, these instability problems may play a dominant role in determining cell efficiency and utility.

All five of these areas of materials properties must be carefully designed and controlled to maximize the efficiency of an actual solar cell. One of the purposes of this book is to describe the ways in which practical considerations of this type have been considered and dealt with.

Reference Information

This book provides three kinds of reference information at the end of the volume: (1) a representative bibliography of books that have been written on the subject of photovoltaics, with entries listed chronologically; (2) a representative list of review papers on aspects of photovoltaics, with entries also listed chronologically; and (3) a traditional list of references to specific research referred to throughout the book by name of author and date of publication, listed alphabetically by first author's name.

In addition, general attention should be called to the published papers presented at a number of meetings dedicated to the subject of photovoltaics. The proceedings of the IEEE Photovoltaic Specialists Conference, with meetings held at 18 month intervals and its 25th meeting in May 1996, are a rich source of information on progress in the field. At this 25th meeting, for example, 370 papers were presented involving almost 1000 authors. The first World Conference on Photovoltaic Energy Conversion met in Hawaii as part of the 24th IEEE Photovoltaic Specialists Conference in 1994, and the Second World

Conference is being held in Vienna in July 1998. There are comparable proceedings of the Photovoltaic Solar Energy Conferences of the Commission of the European Communities; the 14th Conference was held in Barcelona in July 1997.

Another valuable source of continuing input is available through the Program Review Proceedings and the Annual Reports published through the years by NSF-RANN (1973–1975), ERDA (1975–1978), and DOE, and the Solar Energy Research Institute (SERI), now the National Renewable Energy Laboratory (NREL) (since 1978). The Office of Scientific and Technical Information of DOE also published a bimonthly collection of Current Abstracts in Photovoltaic Energy. In 1996 this service was replaced by a listing of abstracts on photovoltaic technology on the World Wide Web at: <http://www.doe.gov/phv/phvhome.html>. Beginning in October 1996, it also became possible to receive a listing of the citations to photovoltaic reports processed by the Office of Scientific and Technical Information (OSTI) during the preceding two months, by regular mail, e-mail, or fax.

Some of the background material included in the book, particularly in this first chapter, is adapted with minor revision from the chapter by the author on “Solar Cells”, in *Handbook on Semiconductors, Device Physics*, Vol. 4, ed. C. Hilsum, 797–839 (1993), with kind permission from Elsevier Science, NL, Sara Burgerhartstraat 25, 1055 KV Amsterdam, The Netherlands. Considerable use has also been made of two other books involving the author for background material and insights into earlier years of research on photovoltaics: *Fundamentals of Solar Cells: Photovoltaic Solar Energy Conversion* by A. L. Fahrenbruch and R. H. Bube, Academic Press, N.Y. (1983), and a chapter on “Photovoltaic Effects” in *Photoelectronic Properties of Semiconductors* by R. H. Bube, Cambridge Univ. Press, Cambridge (1992).

1.2. Applications of Photovoltaics

Photovoltaics are primarily devices to provide alternative sources of electrical energy using the radiant energy that comes to us from the sun. Most of these attempts are motivated by the realization of the limited supply of fossil fuels, the undesirable consequences of nuclear fission, and the stress that energy supply places on the environment in a world with a growing population, a relatively small fraction of which uses far more than its proportional share of energy at the expense of the rest. If the future of the earth is considered in terms of hundreds, rather than tens of years, traditional sources of energy, such as coal, oil and natural gas, provide only a limited resource. Furthermore, growing usage of these fossil fuels contributes to a variety of environmental

problems: air pollution, acid rain, and the greenhouse effect, to name only a few. In principle nuclear energy might be considered as a way to overcome these problems, but nuclear fission is an uninviting prospect in view of the dangers in plant safety, waste disposal, unfavorable economics, and potential for misuse, and nuclear fusion is still an uncertain possibility.

The utility of photovoltaics is especially significant with respect to remote applications, and one of the chief advantages of photovoltaics in the future is decentralization of the power grid, a consideration also related to remote energy use.

A Fundamental Limitation

It should be remembered that there is a fundamental thermodynamic constraint on our ability to convert energy on earth, considering the accompanying heat, without catastrophic effects. If we were to release on earth, through the use of either fossil fuels or nuclear energy, heat corresponding to 1% of the solar power density falling on the earth averaged over a year, the average temperature of the earth would be increased by about 1°C, with major effects on climatic conditions all over the world. Today the average level of energy density consumption in the United States is already about 0.2% of the incident solar power density, with considerably higher values in urban areas. Only renewable energy sources such as solar and wind energy enable us to avoid these constraints.

What Photovoltaic Energy is Available?

Is photovoltaic use of solar energy adequate to the task? Sunlight falls on the earth with an intensity of about 1 kW/m². If this energy could be converted to electricity with a relatively modest 10% overall efficiency, 1 kW of electricity would be generated for every 10 m² of active area as long as the sun was shining near its peak intensity. This is of the order of the average electricity usage per residence. Because the sun does not shine at its peak intensity for 24 hours on any day, and because the periods of sunny days are interspersed with periods of cloudy days, both a greater area than this 10 m² (by a factor of about ten) and a means of electrical storage are required to distribute the use over non-sunny periods.

Main Areas of Concern for Photovoltaics

The basic concerns for long-range use of photovoltaics for terrestrial solar energy conversion lie in three areas: (1) efficiency, (2) cost, and (3) operating

lifetime. These three areas are interrelated in a complex way. Already for a number of years photovoltaics have been applied to a variety of localized tasks, such as pumping water or telephone communications, in developing nations or elsewhere in the world where a power grid does not currently exist. It is the major use of photovoltaics to supply an appreciable fraction of the electrical power on a general basis that raises critical issues.

- (1) The achievable efficiency with a particular photovoltaic system is highly important and it has become generally agreed that cell efficiencies of about 20% (increased from an earlier estimate of 10%) is a lower limit for large-scale power applications. Even if cells with appreciably lower efficiency are very inexpensive, the cost of the cell then becomes insignificant compared to the costs of the installation required for its use. Contemporary efficiencies range from about 14% for single-junction thin-film polycrystalline cells, to close to 30% for single-junction single-crystal cells to be used with solar concentration (up to a factor of 1000 or more). Efficiencies greater than 30% have been achieved with multijunction cells, devices in which the sunlight is passed sequentially through two or more single-junction cells to maximize the match between sunlight absorbed and semiconductor band gap. Most of these cells are made with either silicon (Si) or III-V compounds related to gallium arsenide (GaAs). Only three materials used in single-junction thin-film cells without solar concentration have been demonstrated to provide an efficiency greater than 10%: hydrogenated amorphous silicon (a-Si:H), cadmium telluride (CdTe), and copper indium diselenide (CuInSe₂). Each of these major materials has a chapter devoted to it in this book.
- (2) The basic cost of photovoltaic systems decreased dramatically by a factor of twenty between 1956 and 1976, and in the last decade it has decreased from fifteen dollars to 30 cents per kilowatt-hour; the cost goal by the end of the next decade is six cents per kilowatt-hour. Photovoltaic cells for terrestrial applications will take one of two major forms: a large-area, thin-film, flat-plate form, probably installed at a fixed angle with respect to the earth, suitable for large-area dispersed applications on rooftops etc., or a single-crystal form to be used with a concentrator system built to maintain maximum sunlight on the cell throughout the day through tracking of the concentrator, for centralized power production. Reduction of cost for the thin-film cells is achieved by minimization of the amount of material used, the possibility of inexpensive materials processing methods, and the use of inexpensive mountings. The single crystal cells are themselves generally

- highly complex and expensive, but the small amount of material needed with intense concentration of sunlight again effects a cost reduction.
- (3) To be effective as an alternative energy source, a solar cell must generate at least enough energy in its operating lifetime to pay back both the financial and energy costs required to produce the cell in the first place, and hopefully several times this. It is estimated that an operating lifetime of about 20 years would be a workable value. This lifetime may be determined by a variety of external factors such as physical damage, corrosion, deterioration of cell support structures etc., or by what is of more direct concern to us in this book, by a variety of internal materials-related factors such as diffusion, photogeneration of defects etc. For cells in space, as compared to terrestrial-use cells, radiation damage is also a major factor in degrading performance.

The Illustrative Case of $\text{Cu}_x\text{S}/\text{CdS}$ Solar Cells

Stability for long-term operation has proven to be a real problem for several thin-film technologies. The original all-thin-film, solar cell system consisting of a junction between Cu_xS and CdS showed promise of reasonable efficiency and ease of preparation (Reynolds *et al.*, 1954; Boer and Meakin, 1975; Stanley, 1975; Rothwarf and Barnett, 1977; Barnett, 1977). For a period of almost 20 years, dating from the late '50s, this photovoltaic system was the only all-film cell available. Solar cells with 10% efficiency were also made with $\text{Cu}_x\text{S}/\text{Cd}_{1-y}\text{Zn}_y\text{S}$ thin films ($y = 0.10, 0.16$) with open-circuit voltages greater than that in $\text{Cu}_x\text{S}/\text{CdS}$ cells (Hall *et al.*, 1981). A review is given in Fahrenbruch and Bube (1983) and by Hill and Meakin (1985). Although commonly prepared by the procedure of simply dipping CdS into a warm solution of cuprous ions to effect a replacement reaction in which Cu_xS forms topotaxially on the CdS, other methods of depositing the Cu_xS were also investigated, such as the vacuum evaporation of CuCl followed by heat treatment, or the deposition of Cu_xS by reactive sputtering.

The complexity of this system arises from the variety of Cu_xS phases that may exist at room temperature with quite different photovoltaic properties, and from the ability to change from one phase to another during cell operation due to interaction with the atmosphere or diffusion of Cu into the CdS. Cu_xS can exist in the chalcocite phase ($x = 1.995\text{--}2.000$), which has superior photovoltaic properties, the djurleite phase ($x = 1.96$), and the digenite phase ($x = 1.8$) Reduction in the value of x can occur by diffusion of Cu into the CdS

or by oxidation of Cu at the free surface of Cu_xS , and results in a degradation of photovoltaic properties. Any heat treatment of the cell causes appreciable Cu diffusion into the CdS, which forms deep acceptor states in the CdS that widen the depletion layer and lead to greater carrier recombination before collection, giving rise to *enhanced* (narrow depletion layer), and *quenched* (wide depletion layer) conditions. In addition to these effects, an optical degradation process occurs through a reversible photoinduced defect reaction (Redfield and Bube, 1996), caused by photoexcitation after Cu diffusion into the CdS has occurred (Kanev *et al.*, 1969, 1971). This leads to a state where lifetime-killing defects have been formed that can be thermally annealed away, giving rise to *degraded* (lifetime killer defects formed), and *restored* (lifetime-killer defects annealed away) conditions. In an appropriately heat-treated junction of this type, the value of J_{sc} for the enhanced and restored state (narrow depletion layer and photoinduced defects annealed away), can be over 10^3 times that for the quenched and degraded state (wide depletion layer and photoinduced defects active). The effects associated with the diffusion of Cu into the CdS upon heat treatment used in cell preparation, have been investigated for Cu_xS formed on single crystal CdS (Gill and Bube, 1970; Lindquist and Bube, 1972a,b). Detailed summaries of the results have been described (Fahrenbruch and Bube, 1974, 1983; Bube, 1992).

Many attempts to produce a stable cell in spite of these problems looked promising but proved unsuccessful and further work on the system was finally abandoned, and we will not discuss the details of this particular system further in this book. We refer the interested reader to the above discussions in the literature for what is scientifically a fascinating problem. Among today's thin-film cell materials, stability is a special problem for a-Si:H cells because light-induced formation of defects decreases the lifetime and diffusion length of free carriers; this particular problem remains a live issue and is discussed in more detail in Chapter 3.

1.3. Types of Semiconductor Junctions

There are six different types of semiconductor junctions that have possible application in photovoltaic solar cells, each junction having the fundamental role of supplying the internal electric field needed to separate the photoexcited carriers and to cause them to flow as a current in the external circuit: (1) homojunctions, (2) heterojunctions, (3) heteroface junctions or buried homojunctions, (4) metal-semiconductor junctions (Schottky barriers), (5) *p-i-n* junctions, and (6) semiconductor-electrolyte junctions. We describe the

characteristic energy-band structure for each of these junctions in this section. Discussion of the use of different materials in these possible junction configurations for photovoltaic solar energy conversion makes up the rest of this book.

Homojunctions

A typical energy-band diagram for a homojunction is given in Fig. 1.7. A homojunction consists of a junction between two portions of the same semiconductor, one doped p -type and the other doped n -type, hence the name, p - n junction. Typical details of such an energy-band diagram are shown in the figure: the vacuum level E_{vac} , the conduction band edge E_c , the Fermi level E_F , the valence band edge E_v , the band gap E_G , the electron affinity χ_s , and the diffusion potential $q\phi_D$. The work function $q\phi_W$ of a semiconductor is defined as the energy difference ($E_{vac} - E_F$). Since the work function of the p -type portion of the material is greater than that of the n -type portion in Fig. 1.7,

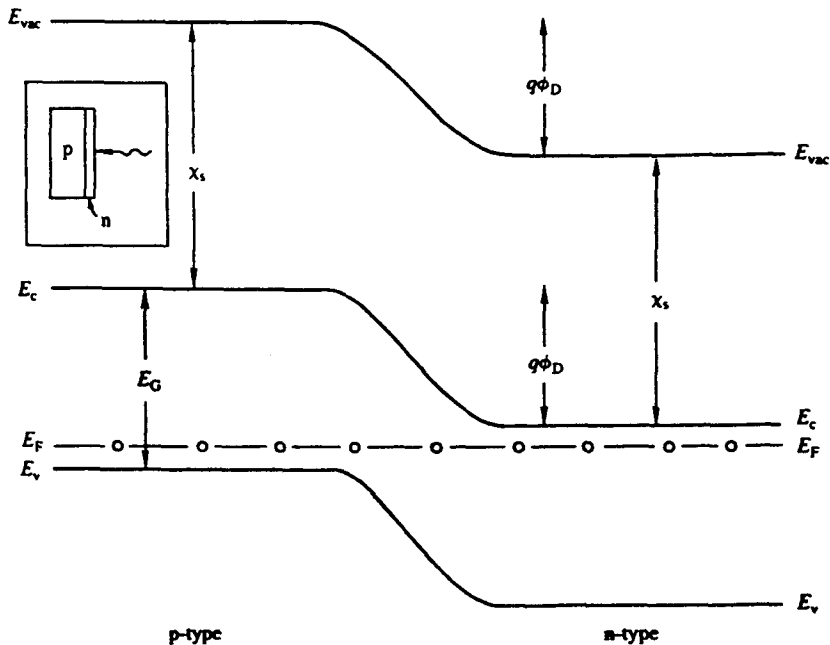


Fig. 1.7. Energy-band diagram for a p - n homojunction with equal densities of doping in the p - and n -type portions.

$(q\phi_{W_p} - q\phi_{W_n}) = q\phi_D$, the energy bands between p - and n -type portions are curved, indicating the presence of an internal electric field. Physically one can think of the diffusion potential $q\phi_D$ as resulting from a transfer of electrons from n -type to p -type material in order to equalize the Fermi energy on both sides when the junction was formed, giving rise to a positive charge of ionized donors in an electron-depleted layer near the junction interface on the n -type side and a negative charge of ionized acceptors in a hole-depleted layer near the junction interface on the p -type side, resulting in a flat Fermi level across the whole structure. The diagram shown in Fig. 1.7 is specifically for the situation where the doping of the p - and n -type regions is the same, resulting in equal widths for the depletion layers on both sides of the junction.

Photoexcitation produces free minority carrier electrons in the p -type region, and free minority carrier holes in the n -type region. Each of these then diffuse toward the junction, and if they reach the junction without being removed by recombination, they pass over the junction, are collected by the junction field, diffuse through the other portion of the semiconductor and pass into the external circuit. Since carriers must be excited within by about a diffusion length of the junction in order to be able to diffuse to the junction before recombination occurs, the geometry shown in the insert in Fig. 1.7 is frequently used, with the portion of the semiconductor on the illuminated side being much thinner than that on the opposite side. If the semiconductor has the high optical absorption characteristic of a direct band gap, then the illuminated side of the junction must be very thin ($\approx 0.1 \mu\text{m}$) to allow light to penetrate to within a diffusion length of the junction, but this has the disadvantage of causing many carriers to be generated near the surface where the probability of recombination due to surface defects is greater than that in the bulk. On the other hand if the semiconductor has a lower optical absorption characteristic of an indirect band gap, then the portion of the semiconductor on the opposite side to that illuminated must be quite thick to allow most of the light to be absorbed, but then much of this absorption occurs more than a diffusion length away from the junction unless the diffusion length of the material is large. These considerations show immediately the need for a high-quality, well-engineered material to serve in an efficient p - n homojunction type of solar cell. High-efficiency, single crystal Si solar cells are usually of the p - n homojunction type.

Heterojunctions

A p - n heterojunction is a p - n junction formed between two different semiconductors with different band gaps and electron affinities. A typical band

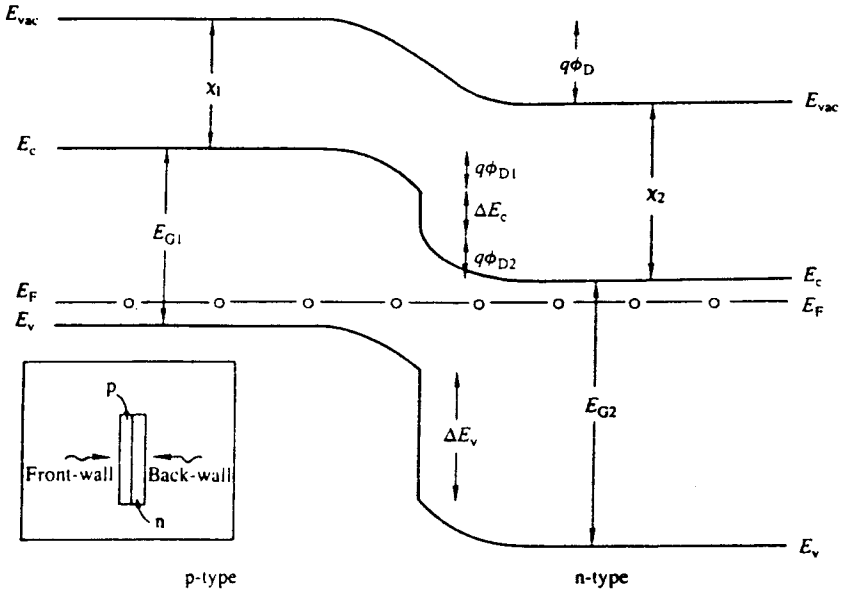


Fig. 1.8. Energy-band diagram for a p - n heterojunction with equal densities of doping in the p - and n -type portions, and a choice of material parameters ($\chi_1 < \chi_2$, $E_{G1} < E_{G2}$) such that there are no energy spikes at the junction interface.

diagram for a p - n heterojunction is given in Fig. 1.8, where the p -type material is assumed to have a smaller band gap E_{G1} than that of the n -type material E_{G2} . As in Fig. 1.7, the assumption is made that the doping is of the same magnitude for both p - and n -type materials, giving equal-width depletion layers on both sides of the junction.

A variety of complex phenomena can occur at the junction interface in such a heterojunction, which we have simplified in Fig. 1.8, following the Anderson abrupt-junction model (Anderson, 1962). In this approach we neglect any effects of interface dipoles or interface states, and recognize that differences between the electron affinities and band gaps of the two material give rise to discontinuities ΔE_c in the conduction band and ΔE_v in the valence band, which can in principle be either positive or negative. Figure 1.8 has been drawn with the desirable assumption that $\chi_1 < \chi_2$, so that an energy spike does not occur in the conduction band impeding electron transport from the p - to the n -type material.

As indicated in the insert in Fig. 1.8, photoexcitation could be either on the n -type material (back-wall) or on the p -type material (front-wall).

Back-wall excitation profits from the larger band gap of the n -type material, which acts essentially like a window even for light that is highly absorbed in the p -type region, and allows the light to penetrate through to the junction with minimum loss. On the other hand, other problems are introduced which are related to the likelihood of lattice mismatch at the junction between the two semiconductors, and which may in itself produce localized interface states that facilitate carrier loss through recombination at what is now a kind of “internal surface”. Such localized interface states may also play a role in increasing the reverse saturation current density J_o and hence reducing ϕ_{oc} .

A typical summary of design choices for materials to be used in a heterojunction is given in Table 1.1.

Table 1.1. Material considerations for use in a heterojunction solar cell.

Property	Criteria
Band gap of smaller band-gap material	Direct gap near 1.4 eV
Band gap of larger band-gap material	As large as possible while maintaining low series resistance
Conductivity type	Smaller band-gap material should be p -type because of longer electron diffusion lengths
Electron affinities	Such that no potential spike occurs at the junction for minority carriers
Diffusion voltage, ϕ_D	Large, since maximum $\phi_{oc} \propto \phi_D$
Diffusion length	Long electron diffusion length in p -type material
Lattice mismatch	Small as possible to avoid interface states at the junction
Electrical contacts	Low-resistance contacts to both n - and p -type materials
Material availability	Good supply of material available
Material cost	Material costs must be competitive
Material toxicity	Materials should be non-toxic, or possible effective control of toxicity
Cell stability	Materials should be free of interactions leading to changes in properties with time or operation

Sometimes a variation on the p - n heterojunction between two semiconductors (sometimes called an SS junction, where ‘S’ stands for ‘semiconductor’) is made by including a thin layer of an insulating material between the two

semiconductors (to form an SIS junction) to help reduce the junction currents that decrease ϕ_{oc} .

Buried Homojunctions or Heteroface Junctions

The energy band diagram of Fig. 1.9 pictures what is called a “buried homojunction” or a “heteroface junction”. It is an effort to benefit from the best properties of a homojunction and a heterojunction, while minimizing their problems. The structure shown consists of a large band gap p^+ -type material which forms a heterojunction to a smaller band gap p -type material, which in turn forms a homojunction with an n -type material with the same band gap. The primary purpose of the structure is to decrease losses due to surface recombination at the illuminated surface in the homojunction configuration by providing the p^+ - p junction with good lattice matching. One of the most successful developments of this type is the p -GaAlAs/ p -GaAs/ n -GaAs cell (Hovel *et al.*, 1972; MacMillan *et al.*, 1988), for which the lattice constant of AlAs is 0.5661 nm and that of GaAs 0.5654 nm; the proportion of Al in the GaAlAs

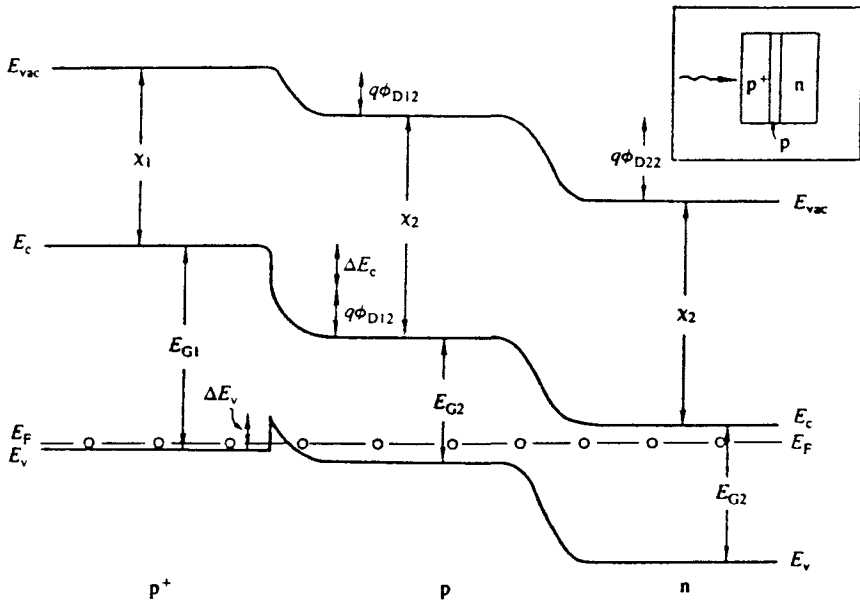


Fig. 1.9. Energy-band diagram for a p^+ - p - n buried homojunction or heteroface junction in which the p^+ material acts as a large band gap window and an ohmic contact to the p -type material. Inset shows the typical direction of illumination for use as a solar cell.

solid solution compound is chosen to provide (a) a large enough band gap to act as a window layer for solar energy, and (b) a good lattice match to the GaAs, hence providing a low interface-recombination velocity at the p^+-p interface.

Schottky Barriers

The previous three types of photovoltaic junctions all involve junctions between two semiconductors. A conceptually simpler junction can be obtained from a Schottky barrier metal contact to a semiconductor (an MS junction).

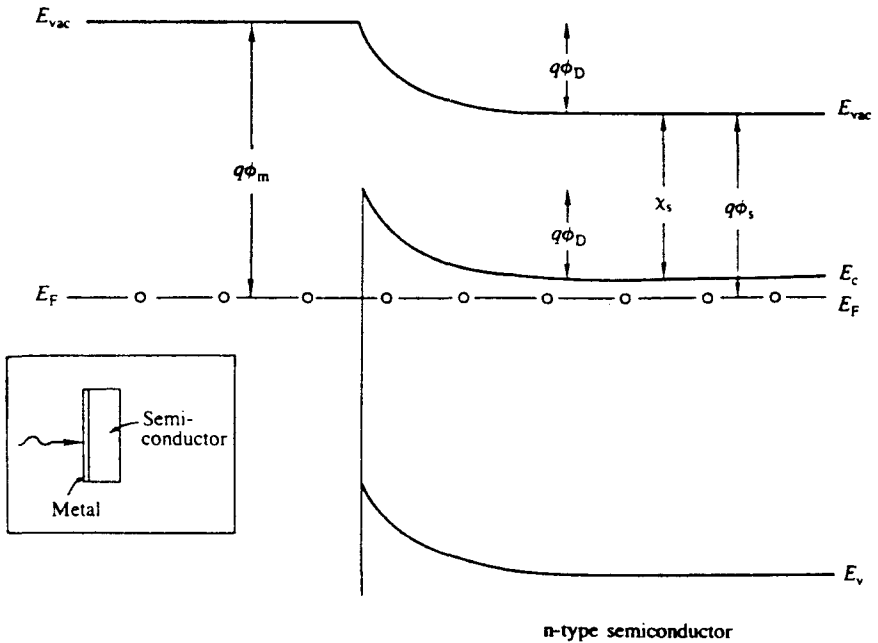


Fig. 1.10. Energy-band diagram for a Schottky barrier metal contact to an n -type semiconductor, based on the energy parameters of the materials without including interface effects.

A typical energy band diagram for a Schottky barrier on an n -type material is given in Fig. 1.10. In the case shown, $q\phi_M > q\phi_S$, and upon contact electrons flow from the n -type semiconductor to the metal, causing a depletion layer in the n -type semiconductor and an internal electric field next to the junction, which is able to collect photoexcited carriers and enable them to contribute to electric current in an external circuit. [For a p -type

semiconductor, a Schottky barrier is formed if $q\phi_M < q\phi_S$, and holes flow from the semiconductor to the metal upon contact, causing a depletion layer for holes next to the junction.] Although a simple approach equates the diffusion potential of the Schottky barrier to the difference between the work functions of the metal and the semiconductor ($q\phi_D = q\phi_M - q\phi_S$), many more complex interactions can occur at the interface that cause variations from such a prediction (e.g. see Fahrenbruch and Bube, 1983). The actual height of a specific Schottky barrier must often be determined experimentally.

Analogous to the case of the SS and SIS junctions, it is frequently found desirable to insert a thin layer of insulator in a Schottky barrier junction to reduce J_o , forming an MIS junction, sometimes referred to as an MOS junction if the insulator is an oxide (Anderson *et al.*, 1977; Stirn and Yeh, 1977). Suitable energy band structures can exist so that the insulator layer reduces the leakage currents of the Schottky barrier, and, as long as it is thin enough not to impede carrier collection, can contribute to improved cell performance.

p-i-n Junctions

What we refer to here as a *p-i-n* junction (see Fig. 3.15 for the energy band diagram of a *p-i-n* junction for a-Si:H) differs from the SIS junction mentioned above in two major ways: (1) the insulator in an SIS or MIS junction is a thin layer confined to the junction region, whereas the insulator in a *p-i-n* junction is usually a thick undoped layer of the same semiconductor where the principal absorption of light occurs; and (2) transport of carriers in an SIS or MIS junction occurs by diffusion between the depletion layer and the contacts, whereas transport in a *p-i-n* junction occurs by drift under an electric field that exists throughout the insulator. Since a collecting electric field exists throughout the region where free carriers are being formed by photoexcitation, there are definite advantages to the *p-i-n* structure. It becomes possible, for example, to use a semiconductor with desirable properties of other kinds but with a diffusion length too small to be useful in a conventional *p-n* structure.

One of the most efficient developments in crystalline silicon solar cells is the *p-i-n* back point-contact (BPC) cell (Swanson *et al.*, 1984) which is discussed in Sec. 2.4. a-Si:H solar cells are usually fabricated in the form of a *p-i-n* junction (Carlson, 1977). An example of a heterojunction *p-i-n* structure is the *n*-CdS/*i*-CdTe/*p*-ZnTe solar cell (Meyers, 1989). Here an *n*-CdS layer is deposited on SnO₂-coated glass, an *i*-CdTe layer is deposited by electrodeposition on the CdS, and a *p*-ZnTe layer is deposited on the CdTe.

Photoelectrochemical Cells

The sixth type of junction goes back all the way to the first discovery of the photovoltaic effect by observing what happens when a semiconductor-electrolyte interface is illuminated. Two types of phenomena are of interest: photoelectrolysis (Bocarsly *et al.*, 1977) and photoelectrochemical cell performance (Gerischer, 1975; Chai *et al.*, 1977; Lewis, 1995). A typical band diagram for photoelectrolysis is given in Fig. 1.11(a), corresponding to the experimental arrangement shown in Fig. 1.11(b), in which electron-hole pairs are excited in a large band-gap semiconductor, which can then be used to dissociate water. A photoelectrochemical arrangement is shown in Fig. 1.11(c), involving an oxidation reaction associated with photoabsorption at one surface and a reduction reaction at another surface, providing a flow of electrons to the external circuit.

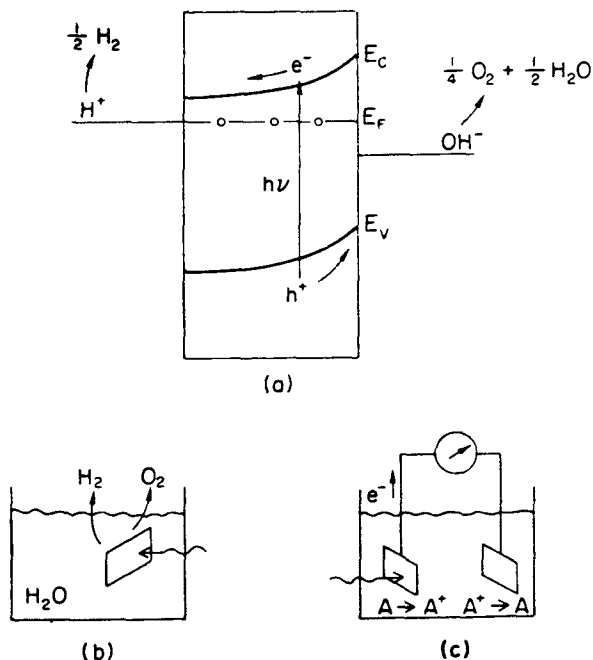


Fig. 1.11. (a) Energy-band diagram for photo-electrolysis using a semiconductor; (b) experimental arrangement for photoelectrolysis using a semiconductor; (c) experimental setup for a photoelectrochemical cell using a semiconductor. (Reprinted from R. H. Bube, "Solar Cells", in *Handbook on Semiconductors. Device Physics*. Vol. 4C. C. Hilsum, ed., 1993, p. 797, with kind permission from Elsevier Science — NL, Sara Burgerhartstraat 25, 1055 KV Amsterdam, The Netherlands.)

1.4. More Detailed Photovoltaic Models

As a first step from the idealized simple model treated in Sec. 1.1 to a more realistic model of a photovoltaic cell, we turn our attention now to several ways of introducing corrections and changes more descriptive of the actual situation.

Three major effects need to be included: (1) effects of $R_s > 0$ and $R_p < \infty$ in Fig. 1.4, (2) voltage-dependent collection effects that make the actual light-generated current density less than J_L , and (3) the possibility of a change in the major parameters J_o , A , R_s and R_p between the dark and light conditions. In the following description, some relatively simple approximations are made to include the consequences of each of these effects.

Differences between Dark and Light Conditions

The single Eq. (1.1) for the junction current in the ideal case must be replaced by two equations, one for the situation in the dark and the other for the situation under photoexcitation. In the dark, we have

$$J^d = \gamma^d \{ J_o^d \exp [\alpha^d (\phi - J^d R_s^d)] + \phi / R_p^d - J_o^d \} \quad (1.8)$$

where the superscript d denotes the dark condition, $\gamma^d = 1/(1 + R_s^d/R_p^d)$, $\alpha^d = q/A^d kT$ for transport mechanisms not involving tunneling, and $\alpha^d = \alpha^{d'}$ for transport mechanisms involving tunneling (as described further below). In the light, we have

$$J^l = \gamma^l \{ J_o^l \exp [\alpha^l (\phi - J^l R_s^l)] + \phi / R_p^l - J_o^l - H(\phi) J_L \} \quad (1.9)$$

where the superscript l denotes the light condition and other definitions are similar to those in the dark. The function $H(\phi)$ is a voltage-dependent collection function that describes what fraction of the light-generated carriers are collected and contribute to the current; we may approximate $H(\phi)$ as follows (Fahrenbruch and Bube, 1974; Mitchell *et al.*, 1977a, b).

Collection Function

For the sake of simplicity, consider a p - n heterojunction with a large band-gap n -type material which transmits photons with energy less than its band gap without loss to the p -type material where they are absorbed. The collection function $H(\phi)$ can be separated into two contributions:

$$H(\phi) = g(\phi) h(\phi) \quad (1.10)$$

Here $g(\phi)$ describes the loss of carriers by recombination in the bulk of the p -type material before they can diffuse to the junction to be collected, and $h(\phi)$ describes the loss of carriers by recombination due to interface states at the junction interface. Qualitatively one would expect that $g(\phi)$ will depend strongly on the photon energy, decreasing for photon energies with lower optical absorption, since carriers are freed further and further from the collecting junction and have an increasing probability of recombining while diffusing to that junction; and that $h(\phi)$ will be relatively independent of photon energy but will depend strongly on the electric field at the interface.

The collection function $g(\phi)$ can be calculated as follows:

$$g(\phi) = \left\{ \int_0^w \exp(-\alpha x) dx + \int_w^\infty \exp(-\alpha x) \exp[-(x-w)/L_n] dx \right\} / \int_0^\infty \exp(-\alpha x) dx \quad (1.11)$$

The dependence of $g(\phi)$ on the photon energy occurs through $\alpha(h\nu)$. The first term in Eq. (1.11) describes the complete collection of all carriers created in the depletion layer with width w , assuming that the drift field there assists in this collection. The second term expresses the possibility of recombination loss of such carriers with increasing distance from the depletion layer if the diffusion length of electrons in the p -type material is L_n . Integration of Eq. (1.11) gives the following expression for $g(\phi)$:

$$g(\phi) = 1 - \exp[-\alpha w(\phi)] / (1 + \alpha L_n) \quad (1.12)$$

which depends on the variation of depletion layer width w with voltage ϕ ,

$$w(\phi) = [2\varepsilon_r \varepsilon_o (\phi_D - \phi) / qN_{D+}]^{1/2} \quad (1.13)$$

where N_{D+} is the density of ionized donors in the depletion layer. As $w(\phi) > 0$, $g(\phi) > 1/[1 + (1/\alpha L_n)]$.

A simple expression for the collection function $h(\phi)$ can be obtained by assuming that recombination at the interface is described by an interface recombination velocity s_I , and that the recombination probability can be considered to be a simple competition between crossing the junction without recombination and recombination at the interface:

$$h(\phi) = 1 / (1 + s_I / \mu \mathbf{E}) \quad (1.14)$$

where μ is the mobility of carriers at the interface, and \mathbf{E} is the electric field at the interface, given by $\mathbf{E} = 2(\phi_D - \phi) / w(\phi)$. If there are N_I interface states

per square centimeter at the interface with a capture coefficient of $\beta_I \text{ cm}^3 \text{ s}^{-1}$, then $s_I = N_I \beta_I \text{ cm s}^{-1}$. The carrier velocity $\mu \mathbf{E}$ must be considered to have a maximum value corresponding to the saturation of drift velocity at high fields.

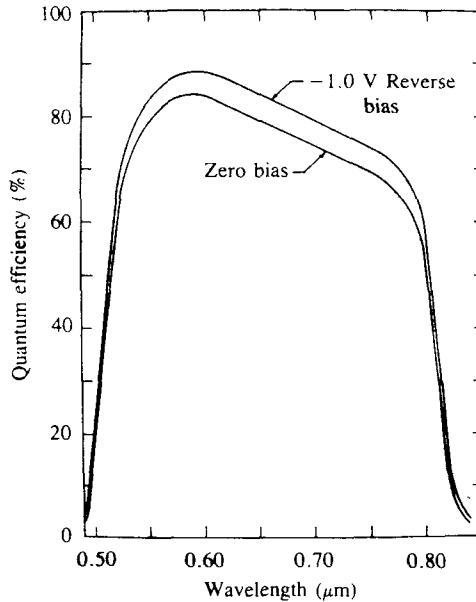


Fig. 1.12. Spectral dependence of the quantum efficiency for an n -CdS/ p -CdTe heterojunction, illustrating the contributions of collection function $g(v)$ (decreasing with increasing wavelength) and $h(v)$ (increasing with applied reverse bias). (Reprinted with permission from K. W. Mitchell *et al.*, *J. Appl. Phys.* **48**, 4365 (1977). Copyright 1977, American Institute of Physics.)

An example of the qualitative effects of these collection functions is given in Fig. 1.12, showing the spectral response of quantum efficiency (density of electrons in external circuit divided by density of photons absorbed) in an n -CdS/ p -CdTe photovoltaic heterojunction (Mitchell *et al.*, 1977b). The short-wavelength cutoff of the spectral response is due to the absorption of shorter wavelengths by the large band gap n -type CdS, while the long-wavelength cutoff is due to failure of the small band gap p -type CdTe to absorb longer wavelengths. The effect of the collection function $g(\phi)$ is seen in the negative slope of the quantum efficiency toward longer wavelengths, with negligible dependence on voltage ϕ . The effect of the collection function $h(\phi)$ is seen in an increase in quantum efficiency with applied reverse bias (thus

increasing E at the interface, and/or decreasing s_I through its own voltage dependence) with negligible dependence on wavelength. Experimental values of $h(\phi) = 0.84$ at $\phi = 0$ and $h(\phi) = 0.89$ at $\phi = -1$ V, indicate a relatively large value of $s_I = 2 \times 10^6$ cm s⁻¹, consistent with the fact that CdS and CdTe have a large 9% lattice mismatch.

Other Photovoltaic Parameters

When the more realistic junction model of Eqs. (1.8) and (1.9) is considered, the other photovoltaic parameters must also be recalculated. For example, the open-circuit voltage becomes

$$\phi_{oc} = (1/\alpha^l) \ln[H(\phi_{oc}) (J_L/J_o^l) + 1 - \phi_{oc}/J_o^l R_p^l] \quad (1.15)$$

and the short-circuit current density becomes

$$J_{sc} = \gamma^l [J_o^l \exp(-\alpha^l J_{sc} R_s^l) - J_o^l - H(0) J_L] \quad (1.16)$$

It can readily be shown that for the relationship between J_{sc} and ϕ_{oc} in this more realistic situation to be the same as the relationship between J^d and ϕ (as was the case in Eq. 1.4), requires seven conditions to be met: γ , R_p , α , and J_o must all be independent of light; $H(0)$ must be equal to $H(\phi_{oc})$; $J^d R_s^d$ must be much less than ϕ ; and $\exp(-\alpha^l J_{sc} R_s^l)$ must be of order unity.

Junction Transport Processes

The parameters J_o and A play critical roles in determining the value of the open-circuit voltage of a solar cell. Simple models of current transport through the junction interface have been developed to indicate some of the significant factors that affect J_o and A in typical idealized cases, and to provide criteria for deciding from experimental data which transport process is active. For simplicity, we use an n^+p heterojunction ($N_D > N_A$, $E_{Gp} < E_{Gn}$) for the following summary of these processes, and illustrate them qualitatively in Fig. 1.13.

Diffusion

The mode of junction transport corresponding to the smallest values of J_o and to $A = 1$ corresponds to a diffusion-controlled current over the junction barrier associated with the injection of electrons [Process (1) in Fig. 1.13] from the n -type material into the p -type material. After injection and diffusion, recombination finally occurs away from the junction in the p -type semiconductor bulk. The current can be expressed as

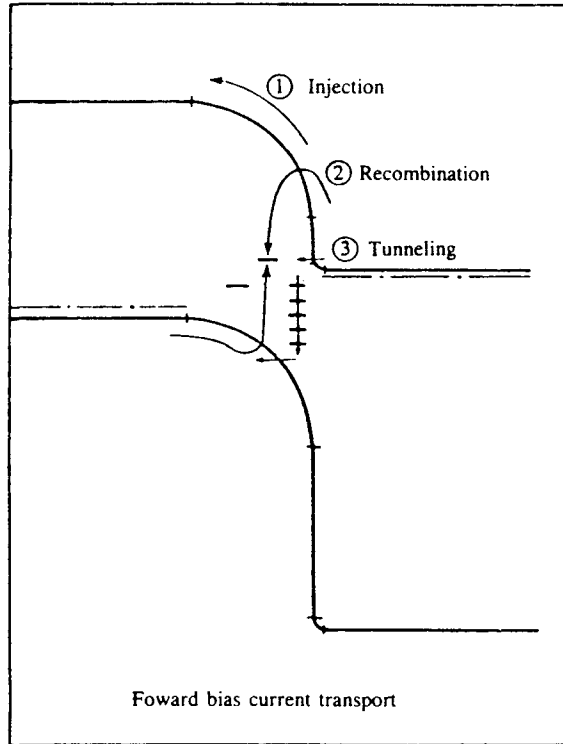


Fig. 1.13. The three major modes of forward junction current transport: (1) injection over the barrier, (2) recombination in the depletion layer, and (3) tunneling, with or without thermal assistance, through interface or imperfection states, followed by recombination. (Reprinted from R. H. Bube and A. L. Fahrenbruch, "Photovoltaic Effect", in *Advances in Electronics and Electron Physics* 56, E. Marton, ed., p. 163. Copyright 1981, Academic Press, Orlando FL.)

$$J_{\text{diff}} = J_o[\exp(q\phi/kT) - 1] \quad (1.17)$$

with $\alpha_{\text{diff}} = q/kT$ and $A = 1$, and

$$J_o = (n_i^2/N_A) q(L_n/\tau_n) \quad (1.18)$$

where, in the p -type material, n_i is the intrinsic carrier density, N_A is the density of acceptors, L_n is the electron diffusion length, and τ_n is the electron lifetime. A plot of $\ln(J_o T^{-7/2})$ versus $1/T$ has an activation energy of E_{Gp} .

Recombination in depletion region

The second smallest mode of junction transport involves recombination in the depletion region [Process (2) in Fig. 1.13]. A recombination rate expression is used based on Shockley–Read recombination (e.g. see Ch. 4 in Bube, 1992), with integration across the depletion regions. The current can be expressed as

$$J_{\text{rec}} = J_o [\exp(q\phi/AkT) - 1] \quad (1.19)$$

with $\alpha_{\text{rec}} = q/AkT$ and $A \approx 2$, and

$$J_o = qn_i [1/(\tau_{no}\tau_{po})^{1/2}] [\pi kT/4(\phi_D - \phi)] w \quad (1.20)$$

where w is the depletion layer width, τ_{no} is the minimum electron lifetime when all recombination centers are empty, and τ_{po} is the minimum hole lifetime when all recombination centers are electron-occupied. The value of A has a maximum value of 1.8 for symmetrically doped junctions if the levels at which recombination occurs lie at mid-gap; otherwise values of A between 1 and 2 may correspond to this mechanism (Sah *et al.*, 1957). A plot of $\ln(J_o T^{-5/2})$ versus $1/T$ has an activation energy of $E_{Gp}/2$. For unsymmetrically doped junctions, the value of A may be equal to or larger than 2 (Choo, 1968).

Interface recombination without tunneling

At an $n^+ - p$ interface, the density of electrons is large and current is limited by the availability of holes, which must overcome the barrier in the valence band. Such currents may be described by

$$J_{\text{int}} = J_o [\exp(q\phi/kT) - 1] \quad (1.21)$$

with $\alpha_{\text{int}} = q/kT$ and $A = 1$. Two conditions may exist: (1) the thermal velocity v_{th} of the electrons is larger than the interface recombination velocity s_I , so that the current is limited by interfacial recombination, in which case

$$J_o = qs_I N_v \exp(-q\phi_D/kT) = qN_I S_I v_{\text{th}} N_v \exp(-q\phi_D/kT) \quad (1.22)$$

where S_I is the electron capture cross-section of interface states with density N_I , and a plot of $\ln J_o$ versus $1/T$ has an activation energy of $q\phi_D$; or (2) the thermal velocity of an electron is smaller than s_I , so that the current is limited by the diffusion of holes to the interface, in which case J_o follows the expression for thermionic emission:

$$J_o = A'T^2 \exp(q\phi_D/kT) = (4\pi qm_h^*/h^3)(kT)^2 \exp(-q\phi_D/kT) \quad (1.23)$$

and a plot of $\ln(J_o T^{-2})$ versus $1/T$ has an activation energy of $q\phi_D$.

Tunneling limited recombination through interface states without thermal assistance

Electrons from the n -type material descend through interface states and then tunnel [Process (3) in Fig. 1.13] through the base of a barrier of height E_b into the valence band of the p -type material. A simple model for this process involves tunneling at the base of a parabolic barrier (Ribben and Feucht, 1966). The junction current in this case is

$$J_{ti} = J_o[\exp(\alpha/kT) - 1] \quad (1.24)$$

with $\alpha = (4\pi/h) (\varepsilon m^*/N_A)^{1/2}$ independent of temperature, and

$$J_o = qp(kT/m^*)^{1/2} \exp(-\alpha v_D) \quad (1.25)$$

so that a plot of $\ln(J_o T^{-1/2})$ versus α has an activation energy of $q\phi_D$.

Thermally assisted tunneling through interface barrier

This model is similar to the last except that holes tunnel through the barrier into electron-occupied interface states at a hole energy enhanced by thermal excitation (Padovani and Stratton, 1966). The current is given by

$$J_{tat} = J_o[\exp(\alpha\phi) - 1] \quad (1.26)$$

with

$$J_o = J_{oo} \exp[-\alpha(\phi_D + E_{fp})] \quad (1.27)$$

with $E_{fp} = E_F - E_v$,

$$\alpha = q/[E_{oo} \coth(E_{oo}/kT)] \quad (1.28)$$

$$E_{oo} = (qh/4\pi) (N_A/\varepsilon m_h^*)^{1/2} \quad (1.29)$$

$$J_{oo} = (\{4\pi qm^*(kT)^2\pi^{1/2} E_{oo}^{1/2} [q(\phi_D - \phi)]^{1/2}\} / \{h^3 kT \cosh(E_{oo}/kT)\} \\ \times [\coth(E_{oo}/kT)]^{1/2}) \exp[-E_{fp}(1/kT - 1/E_o)] \quad (1.30)$$

with $E_o = E_{oo} \coth(E_{oo}/kT)$. This model results in an α that is weakly temperature dependent. A plot of $\ln\{J_o \cosh(E_{oo}/kT) [\coth(E_{oo}/kT)]^{1/2}/T\}$ versus α has an activation energy of $(q\phi_D + E_{fp})$.

Tunneling processes commonly dominate junction currents in heterojunctions, particularly in experimental systems and at lower temperatures. Examples of heterojunctions in which this model appears to appropriately describe

the data include n -CdS/ p -Zn_{0.3}Cd_{0.7}Te (Peters *et al.*, 1988), ZnO/CdTe (Ara-novich *et al.*, 1980), and ZnO/InP (Eberspacher *et al.*, 1984).

1.5. Photovoltaic Materials

The various chapter titles in the remainder of this book indicate the materials that have played a major role in photovoltaic solar energy conversion. Single crystal materials may be useful in high-technology, relatively expensive cells to be used with concentration of sunlight. In single crystal form only Si, GaAs, InP, CdTe and CuInSe₂ can be used in photovoltaic devices to produce efficiencies greater than 10%, and of these only Si and GaAs, and solid-solutions based on them, are considered seriously for terrestrial applications.

This situation calls attention to the importance of thin-film technology in producing thin-film photovoltaic cells for terrestrial applications. In thin-film form, a-Si:H, CdTe and CuInSe₂ are the leading candidates for solar-cell applications. The thin-film technology used must pay particular attention to the processing costs associated with large-area production. Not only are thin films needed for the active solar cell layers themselves, they are also needed for window materials, anti-reflection coatings, passivating coatings, and transparent-conducting contacts (e.g. CdS, ZnCdS, ZnO, SnO, SnO₂, In₂O₃, and indium-tin oxide (ITO)). Decisions have been needed on whether to produce these films by one of the standard methods such as vacuum evaporation, non-reactive or reactive sputtering, electron-beam evaporation, molecular beam epitaxy, and chemical vapor deposition, or by one of a set of developing techniques, such as close-spaced vapor transport (Nicoll, 1963; Saraie *et al.*, 1972; Yoshikawa and Sakai, 1974; Buch *et al.*, 1977), spray pyrolysis (Chamberlin and Skarman, 1966; Ma *et al.*, 1977; Ma and Bube, 1977), and electrochemical deposition or plating (Panicker *et al.*, 1978). The references cited here indicate some of the earlier investigative work; more recent work is described in the following chapters. An assessment of polycrystalline thin films for solar cell applications as of 1982 is summarized by Rothwarf (1982).

Because of the limited number of different materials, research has attempted to broaden the range of possible materials by focusing on solid solutions between these and related materials: e.g. a-Si:C:H, a-Si:Ge:H, Cu_xAg_{1-x}InSe₂, CuGa_xIn_{1-x}Se₂, GaInP₂, Zn_xCd_{1-x}Te, and Mn_xCd_{1-x}Te. Although in principle it is possible to design "ideal" photovoltaic systems with ideal band gap and no lattice mismatch at heterojunction interfaces, by resorting to more complicated ternary, quaternary, pentenary, and even more complex systems, the materials problems entering in these more complex systems appear to be a serious limitation.

A major attempt at increasing efficiency with the limited number of materials available has led to the development of multijunction cells, in which two (or more) different cells are used together in series to more efficiently absorb the light. Although the measured efficiency for such a multijunction cell can be expected to exceed that of either cell used separately, it is clear that efficiencies do not simply add in such a multijunction cell, since only a fraction of the incident light reaches the lower cell. The ideal situation would be to use a large number of such cells in a multijunction such that each cell could effectively absorb light only within a narrow range of its band gap. Examples of early multijunction cells with two components, and the efficiencies achieved are: GaAs/Si (31%) (Gee and Virshup, 1988); GaAs/CuInSe₂ (21.3%) (Stanbery *et al.*, 1977; Kim *et al.*, 1988); AlGaAs/GaAs (24–28%) (Lewis *et al.*, 1988; Virshup *et al.*, 1988; MacMillan *et al.*, 1989); a-Si:H/CuInSe₂ (15.6%) (Mitchell *et al.*, 1988); a-Si:H/a-Si:Ge:H (13.6%) (Guha 1989); GaInP₂/GaAs (25%) (Olson *et al.*, 1989). As we shall see in our later discussions, the structural complexity of even these two-component multijunction cells is often not trivial.